Supplementary materials

Effects of loosely bound electrons and electron-phonon interaction on thermoelectric properties of electrenes

Yi-Ming Zhao,[1] Zishen Wang,[2] Jun Zhou,[3] Chun Zhang,[4,5] Sunmi Shin,[1,*] and Lei Shen[1,†]

[1]*Department of Mechanical Engineering, National University of Singapore, 9 Engineering Drive 1, Singapore 117575*

[2]*Department of NanoEngineering, University of California San Diego, 9500 Gilman Dr, La Jolla, CA 92093-0448, United States 0448*

[3]*Institute of Materials Research and Engineering (IMRE), Agency for Science, Technology and Research (A*STAR) , 2 Fusionopolis Way, Innovis #08-03, Singapore 138634*

[4]*Department of Physics, National University of Singapore, Singapore 117542*

[5]*Department of Chemistry, National University of Singapore, Singapore 117543*

CONTENTS

I. Detailed computational parameters 3

II. Electron transport properties 3

A. Electron and hole mobility 3

B. N-type electron transport properties 3

C. Compared with ZrI_2 5

D. P-type electron thermal conductivity 7

III. Phonon transport properties 8

IV. Temperature effect 9

A. P-type thermoelectric properties 9

B. N-type thermoelectric properties 10

C. Bipolar effect 11

References 13

* mpeshin@nus.edu.sg

† shenlei@nus.edu.sg

I. DETAILED COMPUTATIONAL PARAMETERS

For the structural relaxation of primitive cell, the cut-off energy for wavefunction is 70 Ry under a k-point mesh of 20×20×1. The convergence threshold during self-consistent calculation is set to 10^{-8} eV to ensure an accurate charge density. Both the cell parameter and atom positions are relaxed until the forces get smaller than 10^{-4} eV/Å. For the hybrid functional calculation, the k-point mesh is set to a coarser value of 12×12×1 generated by the kmesh.pl code inside the Wannier90 [1] in order to implemented the subsequent EPW calculation. The q-point sampling of the Fock operator is set as 3×3×1. The phonon calculation is implemented with a q-point sampling of 12×12×1. The dense k- and q-point mesh of EPW is set as 300×300×1. The third order force constant is calculated within the 4×4×1 supercell and the 9th nearest neighbor is considered for the finite displacement calculations. The thermal conductivity calculation is implemented with a 110×110×1 q-point mesh. The AIMD simulation is performed using the 5×5×1 supercell under the micro-canonical (NVE) ensemble.

II. ELECTRON TRANSPORT PROPERTIES

A. Electron and hole mobility

The Fröhlich interaction is quite important for the polar semiconductors with nonzero Born effective charge [2]. The inclusion of interaction between longitudinal optical (LO) phonons and charge carriers decreases the hole relaxation time by almost 10 times as shown in Figure S1a. To validate the electron transport results, we calculate the electron and hole mobility of monolayer HfI_2 as shown in Figure S1b. The hole mobility reaches 4854 $cm^2V^{-1}s^{-1}$ close to the value of 4782 $cm^2V^{-1}s^{-1}$ [3], which indicates our calculations are reasonable. The hole mobility is notably higher than that of the electron, similar to the higher electron relaxation time near the valence band maximum (VBM).

B. N-type electron transport properties

The n-type Seebeck coefficient calculated by only PBE functional is still higher than the other two results with SOI (PBE+SOI and HSE+SOI) similar with p-type case due to the

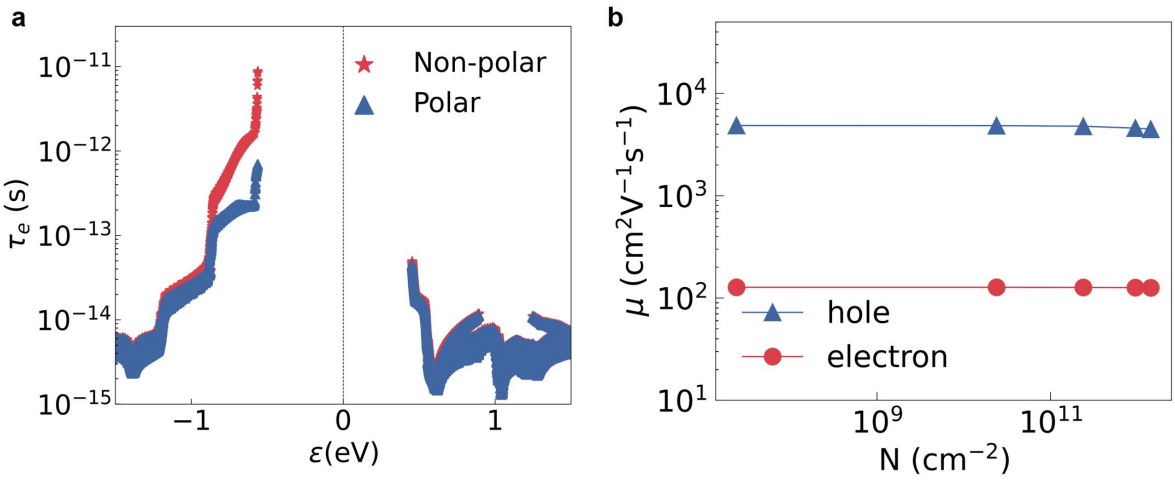

FIG. S1: **a** The carrier relaxation time with and without Fröhlich interaction calculated under HSE+SOI. **b**. The electron and hole mobility at 300K under different doping concentration.

smaller DOS induced by spin splitting as shown in Figure S2a. The Seebeck coefficient of HSE+SOI is close to that of PBE+SOI, although the bandgap of HSE+SOI is larger. The n-type electrical conductivity with SOI are higher than the value without SOI, contrary to the Seebeck coefficient shown in Figure S2b because the electron relaxation time with SOI is obviously higher than without SOI. The power factors are then dominated by the electrical conductivity(see Figure S2c). The peak value of power factor calculated by HSE+SOI is only 1.00 mWm^{-1}K^{-2}, six times smaller than p-type value. The n-type electron thermal conductivity are still proportional to the electrical conductivity as shown in Figure S2d.

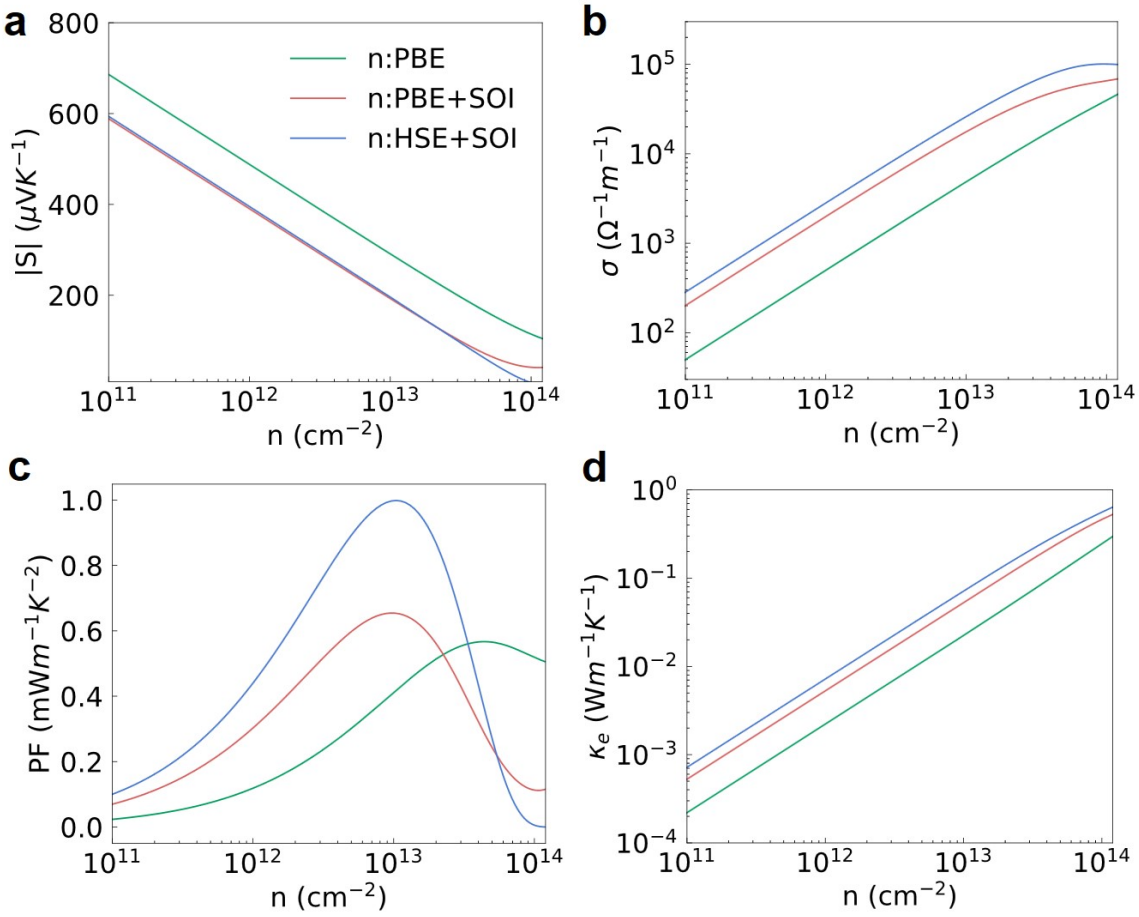

FIG. S2: **a** The absolute value of Seebeck coefficient, **b** The electrical conductivity, **c** the power factor, **d** the electron thermal conductivity under n-type doping calculated by PBE functional, PBE functional with SOI and HSE functional with SOI.

C. Compared with ZrI_2

We also calculated some electron properties of ZrI_2 for comparison. From the band structure calculated by PBE functional in Figure S3a, the electron bandgap of ZrI_2 reaches 0.76 eV close to the bandgap of HfI_2. There are also interstitial electrons at the center of hexagon as shown in Figure S3b similar to HfI_2. The carrier relaxation time of ZrI_2 at valence band maximum under PBE functional is slightly higher than the value of HfI_2 indicating a slightly weaker electron-phonon interaction in Figure S3c, which is consistent with the reported p-type mobility values of ZrI_2 (5138 $cm^2V^{-1}s^{-1}$) and HfI_2 (4782 $cm^2V^{-1}s^{-1}$) [3]. The maximum power factor of ZrI_2 is about 1.5 $mWm^{-1}K^{-2}$ higher than the corresponding

value of HfI_2 in Figure S3d. Overall, there is no large differences in the electron properties of ZrI_2 and HfI_2. The final figure of merit of ZrI_2 will not be larger than the value of HfI_2 due to the higher lattice thermal conductivity of ZrI_2.

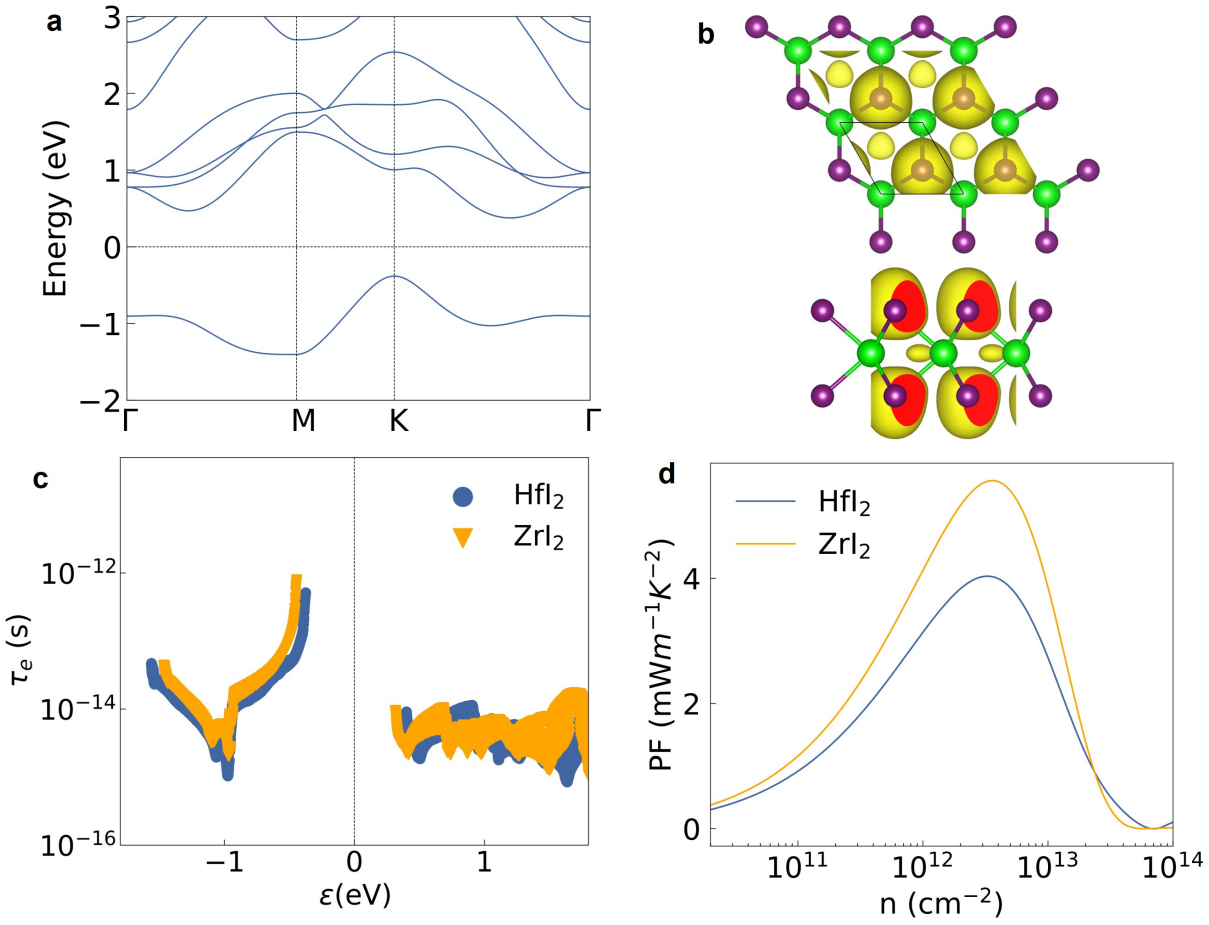

FIG. S3: **a** The electron band structure of ZrI_2 calculated based on PBE functional, **b** The electron localization function with an isovalue of 0.6, **c** the carrier relaxation time of ZrI_2 and HfI_2 under PBE functional, **d** the power factor of ZrI_2 and HfI_2 under p-type doping.

D. P-type electron thermal conductivity

The electron thermal conductivity (κ_e) is obtained directly from the output of BoltzTraP2 [4]. The κ_e results is proportional to the electrical conductivity as shown in Figure S4, which is reasonably consistently with the Wiedemann–Franz law.

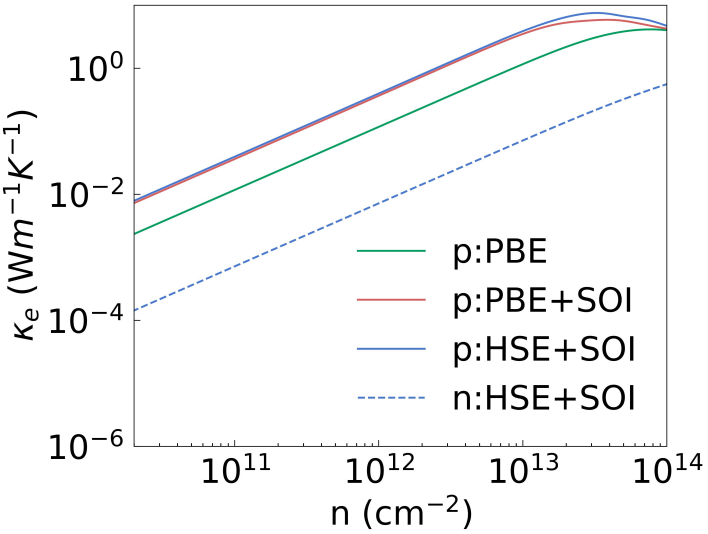

FIG. S4: The electron thermal conductivity calculated by PBE functional, PBE funtional with SOI, HSE functional with SOI under p-type doping. The results of HSE functional with SOI under n-type doping is also plotted in dashed line for convenient comparison.

III. PHONON TRANSPORT PROPERTIES

The scattering rate of low frequency phonons near 50 cm^{-1} from the electron-phonon interaction is higher than that from the three-phonon interaction under electron doping as shown in Figure S5a to c. Then, the lattice thermal conductivity is further calculated utilizing the total phonon scattering rate according to the Matthiessen's rule. The hole doping hardly affect the phonon transport but the electron doping decrease the lattice thermal conductivity obviously (see Figure S5b).

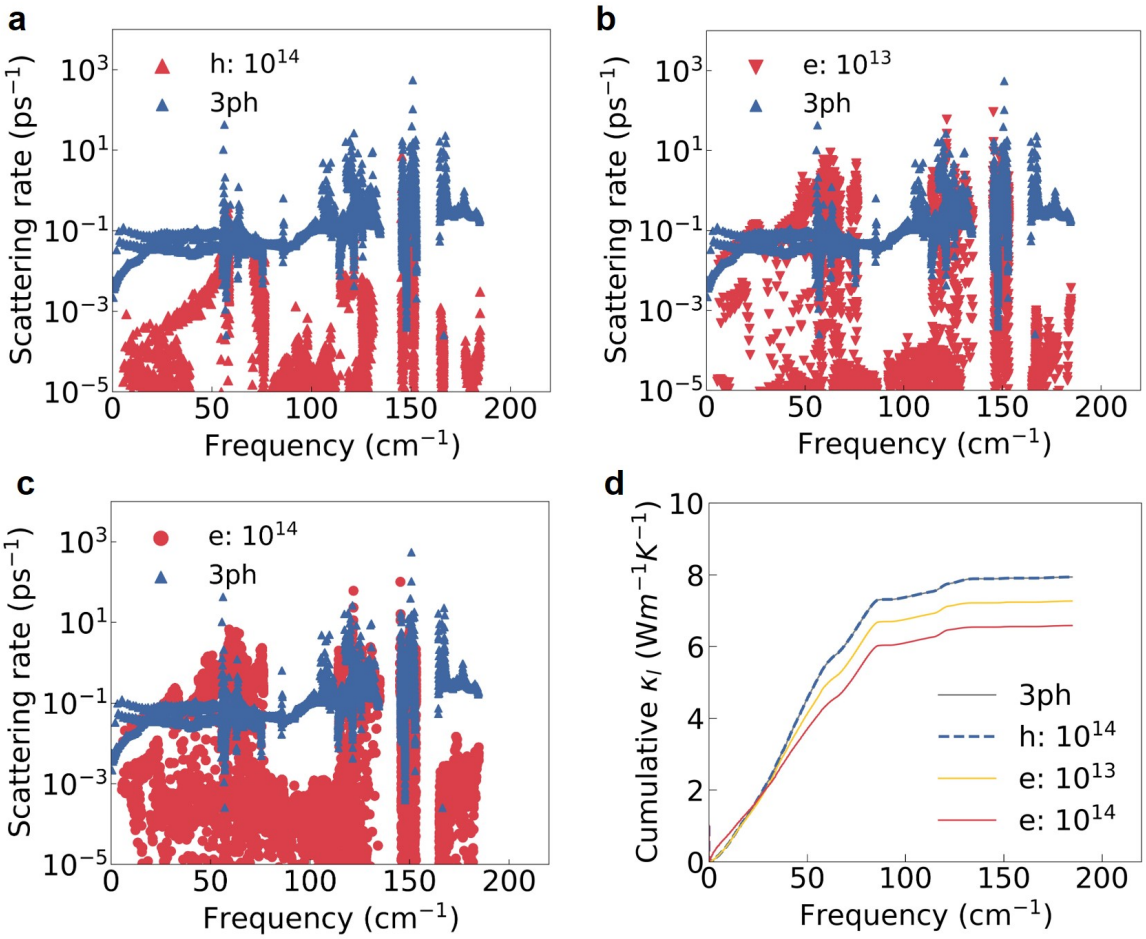

FIG. S5: **a**, **b** and **c** The phonon scattering rate from three-phonon and electron-phonon interaction under different carrier concentration. **d** The lattice thermal conductivity of pristine structure with only three-phonon (3-ph) interaction and doped systems with both 3-ph and electron-phonon interaction.

IV. TEMPERATURE EFFECT

A. P-type thermoelectric properties

Similar to the lower carrier relaxation time at the higher temperature, the mobility also decreases with increasing temperature following an exponential trend as shown in Figure S6a. The Seebeck coefficient gets larger as the temperature increases from 300 K to 1200 K, while the electrical conductivity gets smaller as shown in Figure S6b and c. The electrical conductivity is mainly influenced by the carrier relaxation time. The electron thermal conductivity is still proportional to the electrical conductivity as shown in Figure S6d.

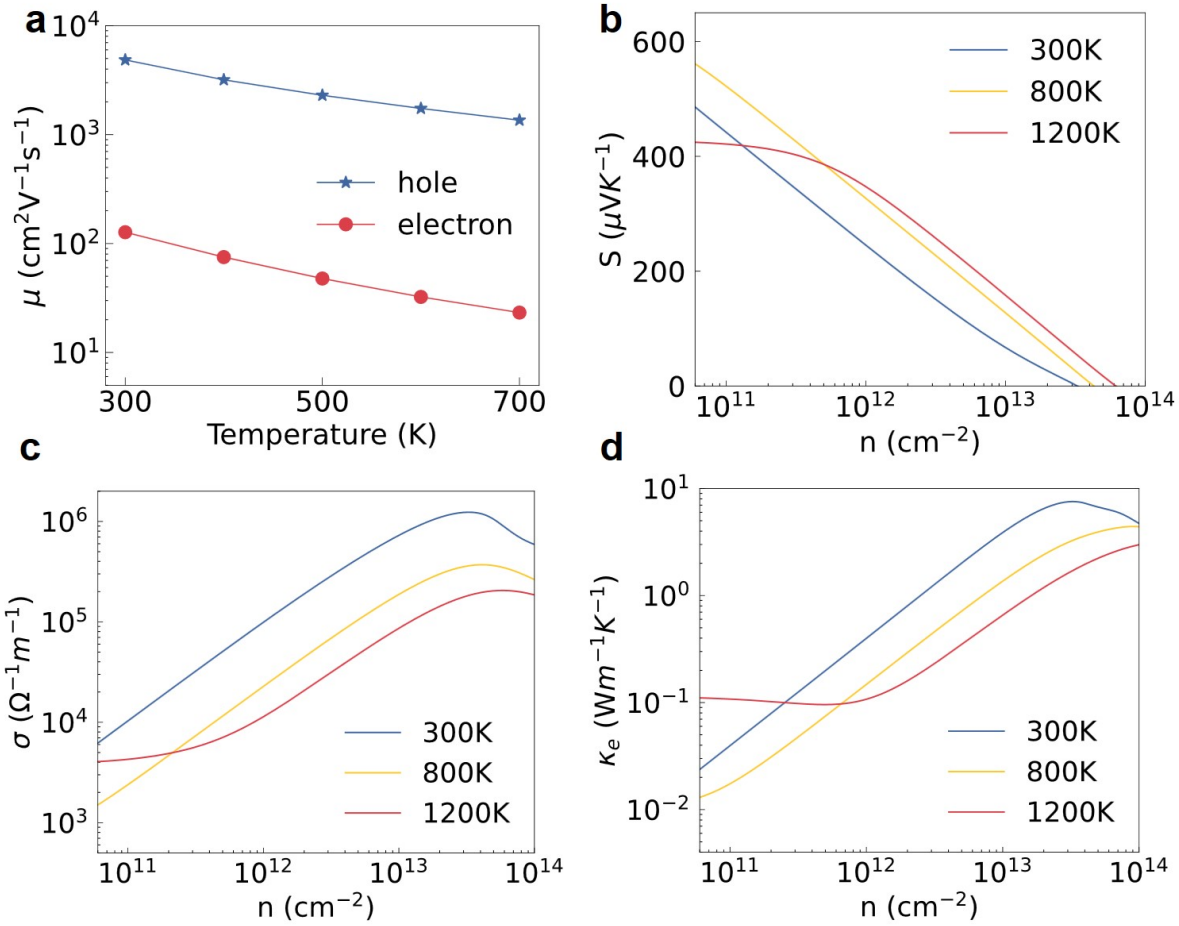

FIG. S6: **a** The variation of electron and hole mobility with temperature. **b** The p-type Seebeck coefficient, **c** the electrical conductivity and **d** the electron thermal conductivity under the temperature of 300, 800 and 1200 K calculated by HSE functional with SOI.

B. N-type thermoelectric properties

For the n-type, the absolute value of Seebeck coefficient increases at higher temperatures. The Seebeck values at 1200K under a doping concentration smaller than 10^{13} cm^{-2} are positive as shown in Figure S7a, indicating a strong bipolar effect [5]. The n-type electrical conductivity and power factor decrease as the temperature increasing in Figure S7b and c. For the temperature of 300 K, the ZT is calculated based on the lattice thermal conductivity under the electron concentration of 10^{13} cm^{-2} where the PF value is largest. At 800 and 1200 K, the ZT value is calculated using the κ_l under the electron concentration of 10^{14} cm^{-2}. The maximum n-type ZT value reaches 0.24 at the temperature of 1200 K under the electron concentration of 10^{14} cm^{-2} as shown in Figure S7d.

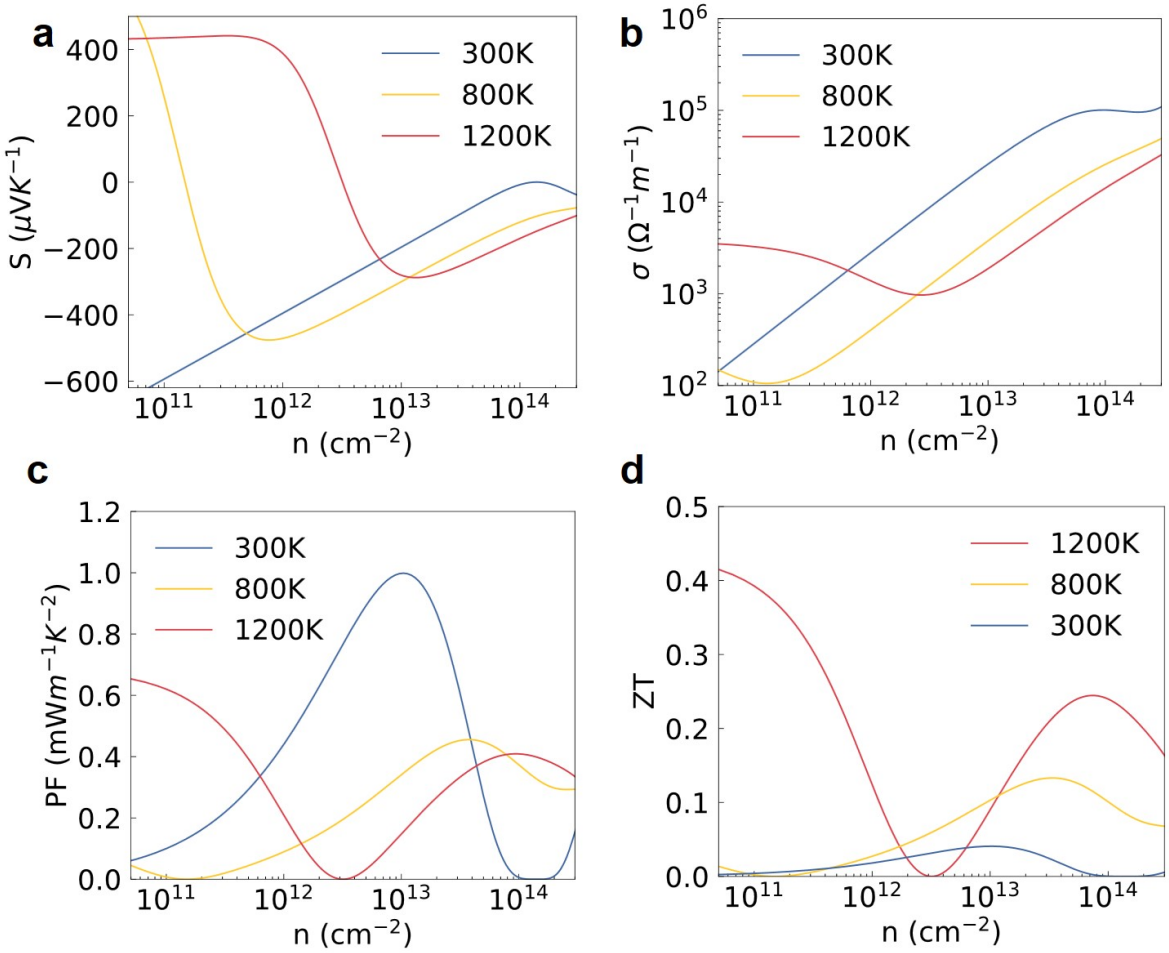

FIG. S7: **a** The n-type Seebeck coefficient, **b** the electrical conductivity, **c** the power factor and **d** figure of merit under the temperature of 300, 800 and 1200 K calculated by HSE functional with SOI.

C. Bipolar effect

The bipolar effect will also increase the thermal conductivity in the thermodiffusion processes, and we further calculate the bipolar thermal conductivity (κ_{bi}) following the formula [6].

$$\kappa_{bi} = \frac{\sigma_{elec}\sigma_{hole}}{\sigma_{elec} + \sigma_{hole}}(S_{elec} - S_{hole})^2 T \tag{1}$$

The total thermal conductivity is calculated by add the lattice, electron and bipolar

thermal conductivity together.

$$\kappa = \kappa_l + \kappa_e + \kappa_{bi} \tag{2}$$

From the results in Figure S8a, the bipolar thermal conductivity is slightly smaller than the p-type electron thermal conductivity. The peak κ_{bi} value is around 0.6 $\mathrm{Wm^{-1}K^{-1}}$ at the concentration of $3{\times}10^{13}$ $\mathrm{cm^{-2}}$. The final p-type figure of merit at 1200 K decreases to 1.12 when the κ_{bi} is considered as shown in Figure S8b.

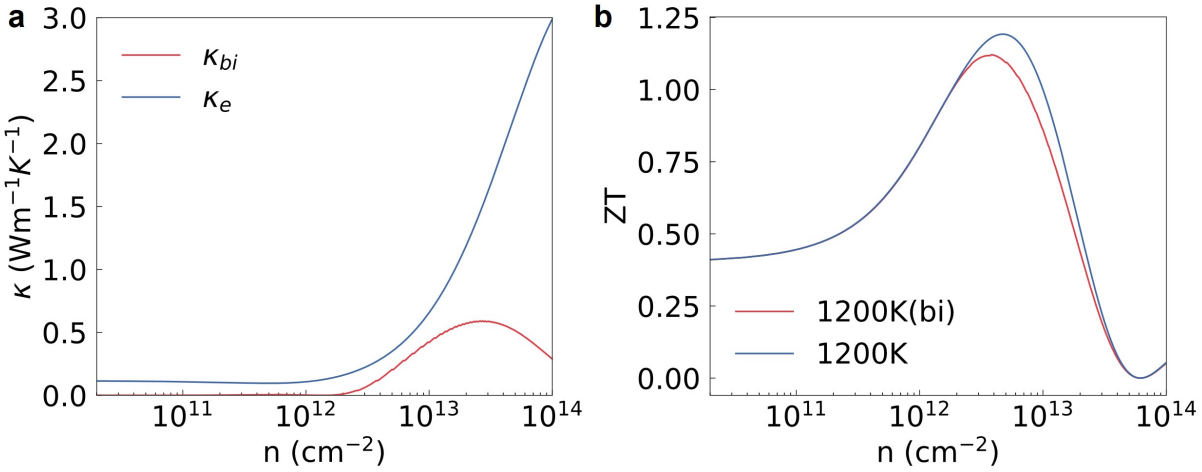

FIG. S8: **a** The electron thermal conductivity under p-type doping and bipolar thermal conductivity at 1200 K. **b** the p-type ZT value with κ_{bi} compared with the one without κ_{bi}.

[1] G. Pizzi, V. Vitale, R. Arita, *et al.*, Wannier90 as a community code: new features and applications, J. Phys.: Condens. Matter **32**, 165902 (2020).

[2] C. Verdi and F. Giustino, Fröhlich electron-phonon vertex from first principles, Phys. Rev. Lett. **115**, 176401 (2015).

[3] C. Zhang, R. Wang, H. Mishra, and Y. Liu, Two-dimensional semiconductors with high intrinsic carrier mobility at room temperature, Phys. Rev. Lett. **130**, 087001 (2023).

[4] G. K. H. Madsen, J. Carrete, and M. J. Verstraete, BoltzTraP2, a program for interpolating band structures and calculating semi-classical transport coefficients, Comput. Phys. Commun. **231**, 140 (2018).

[5] J. J. Gong, A. J. Hong, J. Shuai, L. Li, Z. B. Yan, Z. F. Ren, and J. M. Liu, Investigation of the bipolar effect in the thermoelectric material $CaMg_2Bi_2$ using a first-principles study, Physical Chemistry Chemical Physics **18**, 16566 (2016).

[6] J.-H. Bahk and A. Shakouri, Enhancing the thermoelectric figure of merit through the reduction of bipolar thermal conductivity with heterostructure barriers, Appl. Phys. Lett. **105**, 052106 (2014).